Parametric Study of Structured Thermocline Storage Systems

Jordi Vera[1], Oriol Sanmartí[1], Santiago Torras[1], Carlos D. Perez-Segarra[1]

[1] Heat and Mass Transfer Technological Center, Technical University of Catalonia. Carrer de Colom 11, 08222 Terrassa (Barcelona), Spain.

Abstract

A thermal accumulator system for concentrated solar power is modeled to perform a parametric study. The thermal accumulation system is a type of structured thermocline where there is a solid filler material with some channels where the heat transfer fluid (HTF) circulates. The energy is accumulated in both the HFT (a molten salt) and the solid (a ceramic material). The model considers a simplified 3D domain for the solid, considering a single channel and taking advantage of the symmetries of the problem. For the fluid, a 1D step-by-step discretization is used, and the solid and fluid are coupled using a conjugate heat transfer (CHT) approach. The studied parameters are geometrical parameters (tank diameter, tank height, channel diameter, distance between channels, and channels arrangement) and operational parameters (charge and discharge cycles criteria, mass flow rates).

Keywords: Concentrated Solar Power, Thermal Energy Storage, Thermocline, CFD

1. Introduction

Solar towers are a type of solar renewable energy that consists of redirecting the direct solar energy from a set of mirrors, heliostats, to a small region, the receiver. These elements make up the solar field. The receiver has a circulating heat transfer fluid (HTF), generally a molten salt, that transports some of the thermal energy to a power block to generate vapor. The remaining thermal energy is stored in a thermal energy storage (TES) tank. The energy from this storage tank is used to power the turbine when needed (e.g., at night).

The traditional thermal storage consists of a two-tank system (Pelay et. al., 2017), where the high-temperature molten salt is stored in one tank, and the low-temperature molten salt is stored in the other one. An alternative storage system is using a single thermocline tank. Thermocline systems work with a porous filler material where the fluid can freely move, and the energy is stored on the solid filler material and the fluid. More information on these types of systems can be seen in (Galione et. al., 2015) and (Gonzalez et. al., 2016). A variant of this type of system is to consider that the filler material is arranged in a structured pattern, where the solid is a continuous material with some channels or tubes where the HTF can circulate. In this work, the structured variant will be studied.

2. Case geometry and operation conditions

A schematic representation of the studied storage tank is shown in Figure 1. It consists of a solid material called the bed, which has some drilled or manufactured channels inside. A molten salt flows inside the channels. To give an idea of the orders of magnitude of the studied case, the diameter of the tank is at the order of $D_{tank} \sim 45\ m$, its height is at the order of $H \sim 13\ m$, and the channels have a diameter of approximately 1 cm. In this particular case, the number of channels in the tank is greater than 4 million.

These channels/holes can be arranged in different geometrical patterns. One parameter that can be modified is the diameter of the channels, another parameter is the distance between channels, and finally how these channels are arranged. In the studied case, two channel arrangement are considered, one where all the tubes are in line (square arrangement) and another one where the tubes are staggered (triangular arrangement, as seen in Figure 1).

In addition to the HTF inside the channels, the tank has also bottom and top buffer zones with the HTF. The bottom part of the tank has molten salt at a low temperature ($T_d \sim 300\ ºC$) while the top of the tank has hot molten salt at a high temperature ($T_c \sim 565\ ºC$). The physical and thermal properties of the molten salt are taken from (Bonk et. al., 2018) and are temperature dependent. Therefore, this has to be considered in the analysis. The studied molten salt can have up to 10% variation in density due to temperature changes, so for a fixed mass, the volume will change. This change of volume occurs at the top buffer zone, where its free surface can move up and down to compensate for these changes in density.

doi:10.18086/eurosun.2022.13.22 Available at http://proceedings.ises.org

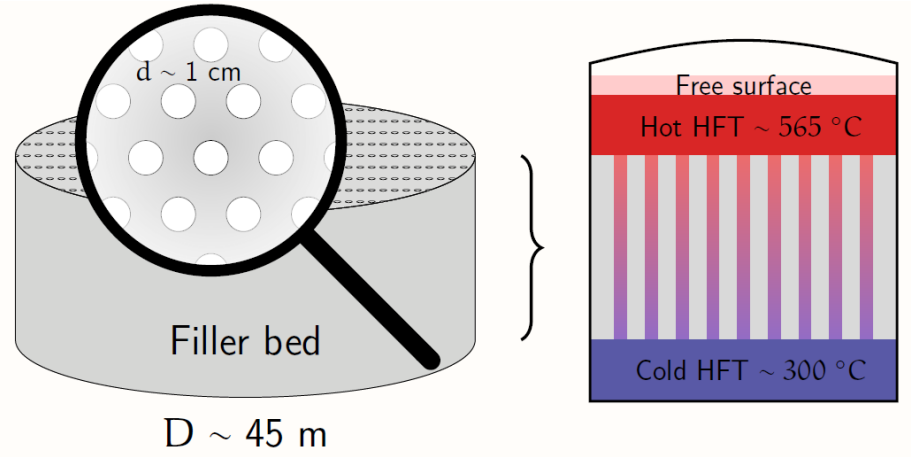

Fig. 1: Geometry of the filler bed (left) and the overall tank (right).

The working regime of the tank consists of two operational modes, one of charging (Figure 2, left) and the other of discharging (Figure 2, right). In the charging operation regime, the energy from the solar field heats the fluid (molten salt) that circulates downwards the storage tank, increasing the temperature of the solid filler material. In the discharging process, the molten salt circulates upwards and the energy stored is delivered to the fluid that goes to the power block to generate vapor.

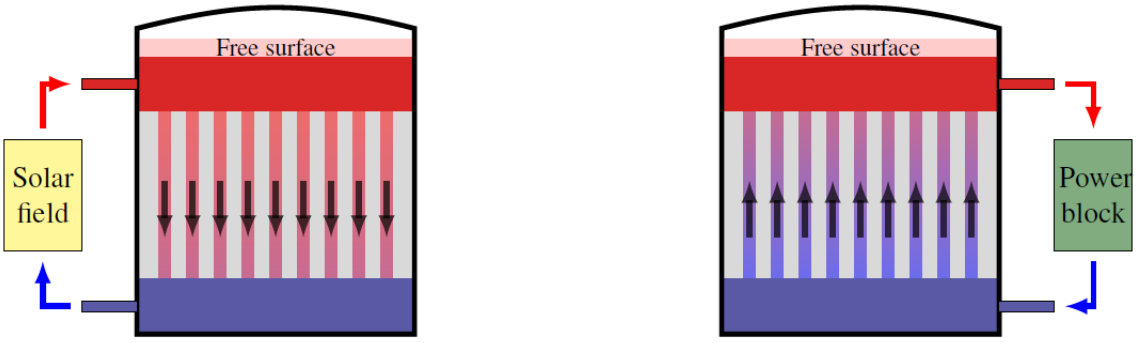

Fig. 2: Operation regimes of the tank. Charging process (left) and discharging process (right). Source: (Vera et. al., 2022).

In the case of our study, the behavior of the system over different cycles is evaluated, with particular emphasis on the case where it has reached a stationary cycling condition (once there is no significant difference between consecutive charging and discharging cycles). A cycle (shown in Figure 3) starts with the charging process. The solar field provides heated HTF from the top, and this HTF circulates from top to bottom heating the solid bed. Once the bottom buffer zone of the tank reaches a certain cutoff temperature increment $\Delta T_{co}^{(c)}$, the HTF stops circulating and the tank enters an idle mode over some prescribed time $t_{id}^{(cd)}$ (in the evaluated cases of this work this idle time is zero for both charging and discharging modes). After this idle period, the tank starts the discharging mode. The "cold" HTF circulates from bottom to top, and it gets heated with the energy from the solid bed of the tank. The HTF at high temperature of the top is then used to supply the power block. The process continues until the top buffer zone reaches a temperature drop greater than the cutoff temperature $\Delta T_{co}^{(d)}$, then the mass flow stops, the tank enters some idle cycle for some time $t_{id}^{(dc)}$ and then the charging process starts again and the cycle is repeated. In the simulation, several cycles are simulated until a cycling steady condition is reached.

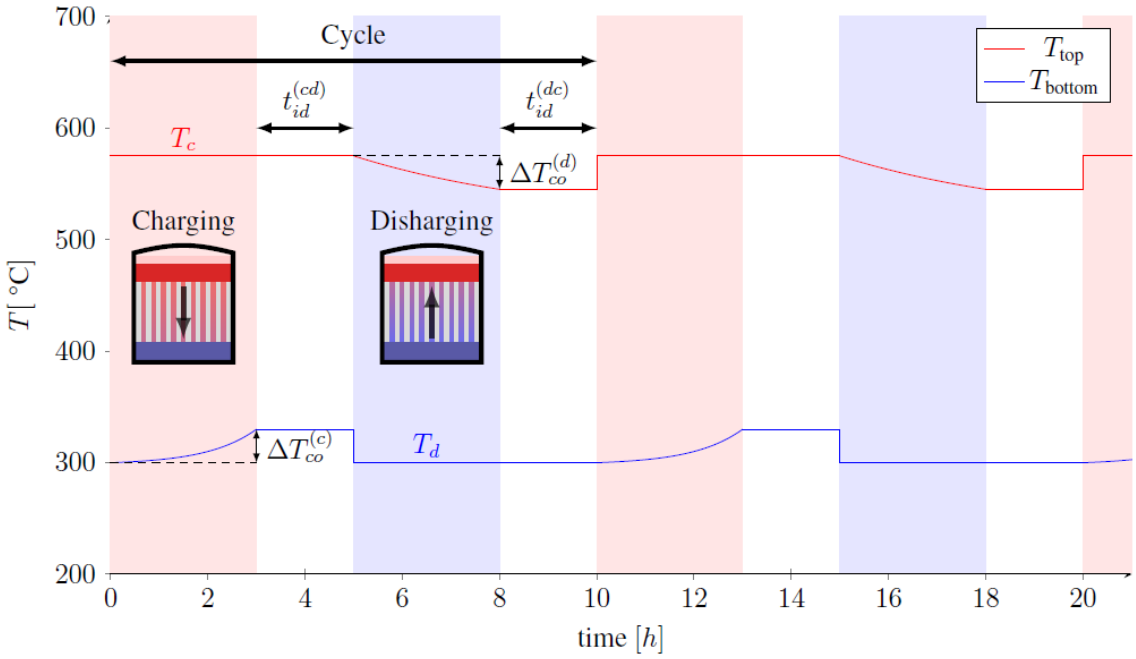

Fig, 3: Charging and discharging cycles for the thermocline. Source: (Vera et. al., 2022).

3. Methodology

The study of heat transfer is done using a conjugate heat transfer (CHT) approach. Assuming uniform flow distribution and negligible heat losses to the ambient, a basic cell of the domain is fully modeled. The selected region of the solid and fluid is shown in Figure 4. The computational domain is then chosen considering the planes of symmetry, and assuming that the inner tubes behave equally due to this symmetry.

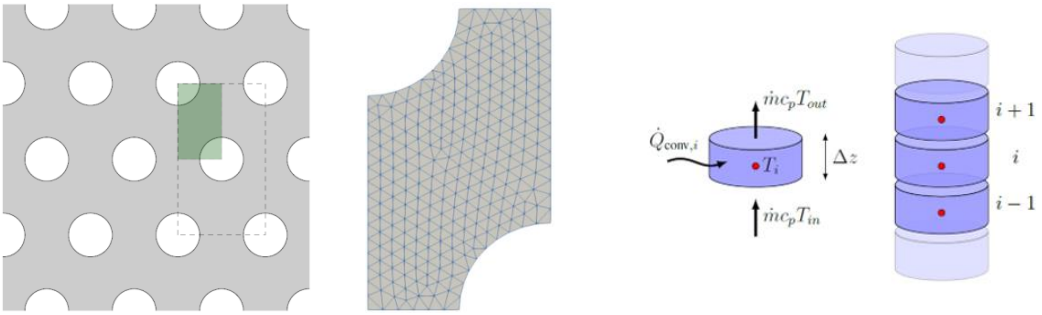

Fig. 4: Domain and meshing of the solid (left) and fluid (right).

The solid is discretized with a 3D extruded mesh. The conduction heat transfer equation (eq. 1) is solved by employing a finite volume approach, considering adiabatic boundary conditions for the walls at the symmetry planes, and a coupled convection boundary condition for the tube walls in contact with the fluid.

$$\rho_s c_{ps} \frac{\partial T}{\partial t} = \nabla \cdot (k_s \nabla \mathrm{T}) \qquad \text{(eq. 1)}$$

In the periodic faces, an adiabatic boundary condition $\dot{q} = 0$ is imposed.

The fluid is discretized using a 1D mesh. The continuity (eq. 2) and energy (eq. 3) equations are numerically solved with the Finite Volume Method (FVM).

$$\frac{\partial \rho_f}{\partial t} + \nabla \cdot \boldsymbol{v} = 0 \qquad \text{(eq. 2)}$$

$$\rho_f c_{pf} \left(\frac{\partial T}{\partial t} + \boldsymbol{v} \cdot \nabla T \right) = \nabla \cdot \left(k_f \nabla \mathrm{T} \right) \qquad \text{(eq. 3)}$$

For the continuity equation, the mass that enters and exits the domain are equal and imposed as boundary

conditions, and the height of the buffer zone at the top is calculated at each time iteration.

For the energy equation, the temperature is imposed at the top (for the charge cycle) or bottom (for the discharge cycle). For the charge cycle, the temperature is imposed at the top with T_c, while for the discharge cycle the temperature is imposed at the bottom with T_d.

The momentum equation is also solved to evaluate the pressure losses over the tubes, however, given the low speed and Reynolds number of the HTF inside the channels (order of magnitude of $v \sim 2$ mm/s and $Re \sim 18$), the pressure losses were shown to be mainly due to the change of potential energy of the HTF from bottom to top ($\rho g \Delta h$), while the other terms were negligible.

The time scale of the case is in the order of hours or even days, so a large timestep is needed to compute the case with affordable computational resources. Therefore, the solid and the fluid are discretized using an implicit approach to allow large timesteps. The CHT coupling between the solid and the fluid is done using a semi-implicit approach. More information on the model is shown in (Vera et. al., 2022)

A reference case with fixed parameters is defined (see Table 1). Then a parameter is chosen and this parameter is changed keeping the other parameters equal to the reference case. The studied parameters can be either geometrical changes (channel diameter, distance between channels, channel arrangement, tank diameter/height) or operational changes (mass flow rate, cutoff temperature).

Regarding the channel's geometry and arrangement, the influence of changing the diameter d, the distance between tubes L_{tp}, and their arrangement (either an inline arrangement or a staggered one) are studied. Figure 5 shows a schematic of the variation of the geometry of the channel.

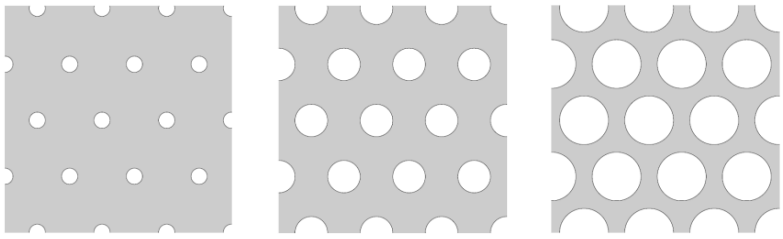

a) Channel diameters of 5mm, 10mm, and 15mm (from left to right).

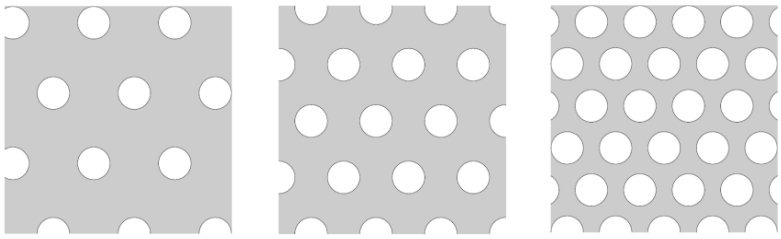

b) Distance between channels of 25mm, 20mm, and 15mm (from left to right).

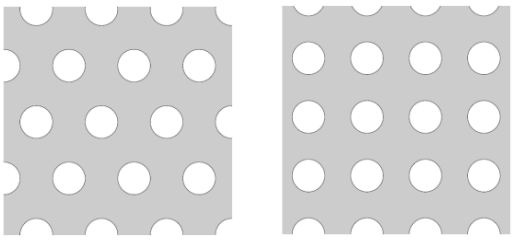

c) Channel arrangement, triangular 30° (left) and square 90° (right).

Fig. 5: Changes in the distribution and geometry of the channels .

The influence of the overall geometry of the tank is also studied. Figure 6 shows the variations in the tank

dimensions. The objective is to change the dimensions maintaining the bed volume constant, meaning that a change in the diameter will result in a change in the bed height. Given that the change in diameter influences the quantity of molten salt at the buffer zones (bottom and top), two ramifications of the cases are considered; maintain the top and bottom height, meaning that the volume of molten salt will change (see left Figure 6) or maintain the volume of molten salt and change the height (see right of Figure 6).

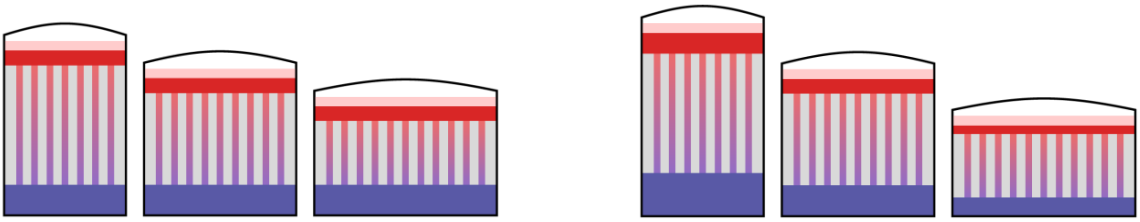

Fig. 6: Changes in the diameter and height of the tanks keeping the buffer zones height constant (left) and keeping the buffer zone volume constant (right).

The operational parameters that are studied are the cutoff temperature and the charge/discharge mass flow rate. The larger the cutoff temperature variation, the longer the duration of the cycle, so more energy is accumulated. For the mass flow, it would be expected that a high mass flow (maintaining the same geometry) increments the velocity of the molten salt, reducing the time cycle.

A summary table of all the cases and changed parameters are shown in Table 1.

Tab. 1: Summary of the values used for the parametric study (reference case in bold)

Parameter	Value	
Tank Diameter | Bed height (D_{tank} | h_{bed}) with constant bed volume and constant buffer zones height	39.40 m | 15.0 m **45.00 m | 11.5 m** 48.25 m | 10.0 m 53.95 m | 8.0 m	
Tank Diameter | Bed height (D_{tank} | h_{bed}) with constant bed volume and constant buffer zones volume, variable (h_{top} | h_{bottom})	39.40 m | 15.0 m **45.00 m | 11.5 m** 48.25 m | 10.0 m 53.95 m | 8.0 m	1.30 m | 0.65 m **1.00 m | 0.50 m** 0.87 m | 0.43 m 0.70 m | 0.35 m
Tube diameter d	5 mm **10 mm** 15 mm	
Distance between tubes L_{tp}	15 mm **20 mm** 25 mm	
Hole arrangement (constant d and void fraction)	**30º (Triangular)** 90º (Square)	
Cutoff temperature ΔT_{co}	**15 ºC** 30 ºC 45ºC	
Charge/Discharge mass flow ($\dot{m}_{charge}$ | $\dot{m}_{discharge}$) (Constant geometry)	744 kg/s | 307 kg/s **1488 kg/s | 615 kg/s** 2976 kg/s | 1230 kg/s	

4. Reference case results

For the reference case, the accumulated energy is 1311 MWh, with a charge cycle of 2.1 h of duration, and a discharge cycle of 5.1 h. It should be noted that the accumulation capacity of the thermocline storage tank is not the same at the first cycle as once it has performed multiple cycles. This behavior is shown in Figure 7. The thermocline solid bed starts all at 300 ºC and has greater accumulation capacity, and with each cycle, it loses some storage capacity until a steady state of accumulation capacity is reached.

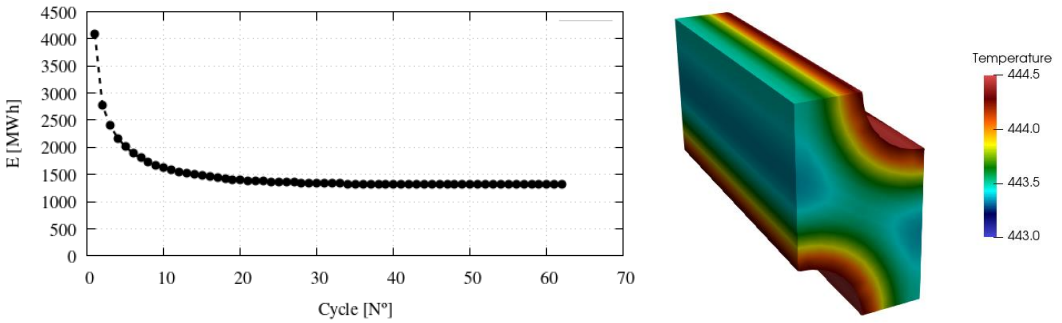

Fig. 7: Evolution of overall accumulated energy as a function of the cycle (left) and detailed temperature distribution on a region of the solid (right).

The solid bed can be studied in detail with the presented model. Figure 7 shows the instantaneous temperature distribution of the solid at some height of the channel in the cycle of charging. It can be seen that the difference between the hottest and coldest part of the solid in that section is less than 2 ºC. The solid accounts for 77% of the energy accumulation while the molten salt accounts for the remaining 23%.

The temperature distribution of the fluid over time can also be studied with the presented model. Figure 8 shows the temperature distribution of the HTF on different time instants for the charge and discharge cycles. The profiles are quite similar despite having different durations due to the difference in mass flow rates for the charge and discharge.

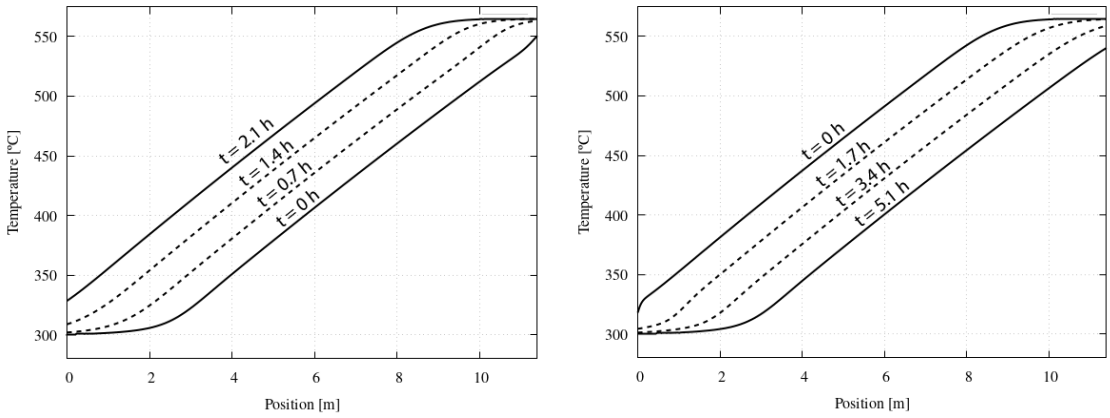

Fig. 8: Axial temperature distribution of the HTF for charging (left) and discharging (right) cycles over time.

For a fixed time instant, the HTF temperature could be approximated to a linear profile. In order to understand the duration of a cycle and the strong influence of the different parameters, let's introduce a simplified case. A perfect temperature linear profile is assumed, where the mass flow transport of the HTF is much greater than its heat convective losses. Another assumption is that there is no top or bottom buffer zone, so the cutoff criteria will be evaluated when the HTF is exiting the channels. The fluid temperature profile in this case would be similar to the one shown in Figure 9.

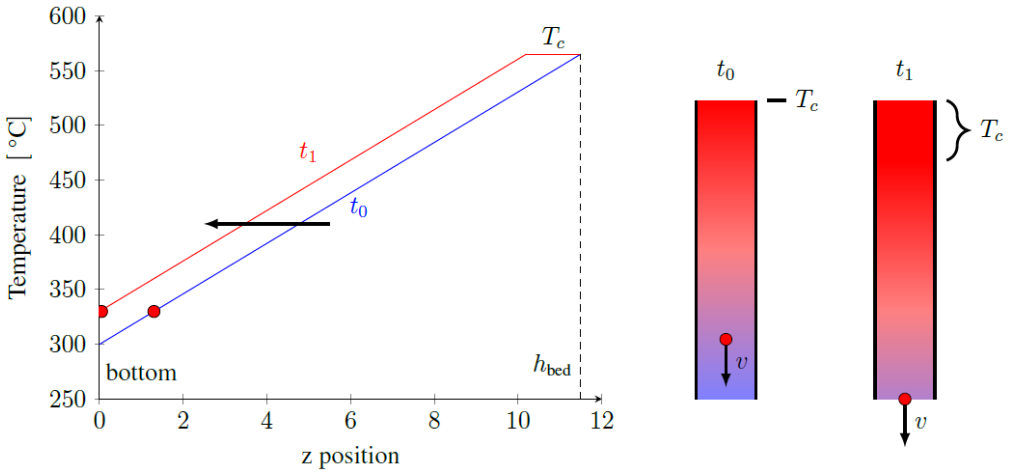

Fig. 9: Evolution of a linear fluid temperature profile over time.

The linear temperature distribution makes a translation over time. The temperature at the top has a fixed value (so a constant temperature is transported in this case). It can be seen that the velocity at which the plotted line moves is the speed of the fluid in the tubes. There is a strong dependence on the velocity of the HTF and the duration of the cycle, which affects the accumulation of energy. Furthermore, the power of the cycle seems to significantly change only with the mass flow rate.

If the buffer zone is neglected, the mean power of a cycle can be calculated with eq.4.

$$\bar{P} = \frac{\int_0^{t_{cycle}} \dot{m} c_p (T_{in} - T_{out}(t))\, dt}{\int_0^{t_{cycle}} dt} \qquad \text{(eq. 4)}$$

Considering a linear profile behavior for $T_{out}(t)$, eq. 5 expression is obtained.

$$\bar{P} = \dot{m} c_p \left((T_c - T_d) - \frac{\Delta T_{co}}{2} \right) \qquad \text{(eq. 5)}$$

Although in reality the temperature profile is not exactly linear and the results might change a bit, this gives an idea of the parameters that have more influence over the charge and discharge power, which are the temperature differences, the mass flow rate, and the cutoff temperature (although this last one has less influence).

The implication of this is that given a fixed mass flow rate, the accumulated energy will be almost proportional to the duration of the cycle. The duration is determined by how fast the outlet reaches an increment or decrease of the cutoff temperature. The worst-case scenario would be if the heat transfer from the fluid to the solid was very poor, so the fluid would not be able to transfer energy and the duration of the cycle would decrease, storing less energy. The ideal scenario would be that the heat transfer is very efficient, meaning that the fluid takes longer to reach the cutoff temperature because the heat gets dissipated to the solid, so the cycle is longer and the heat accumulated is increased. The two fluid temperature profiles of these hypothetical cases are shown in Figure 10.

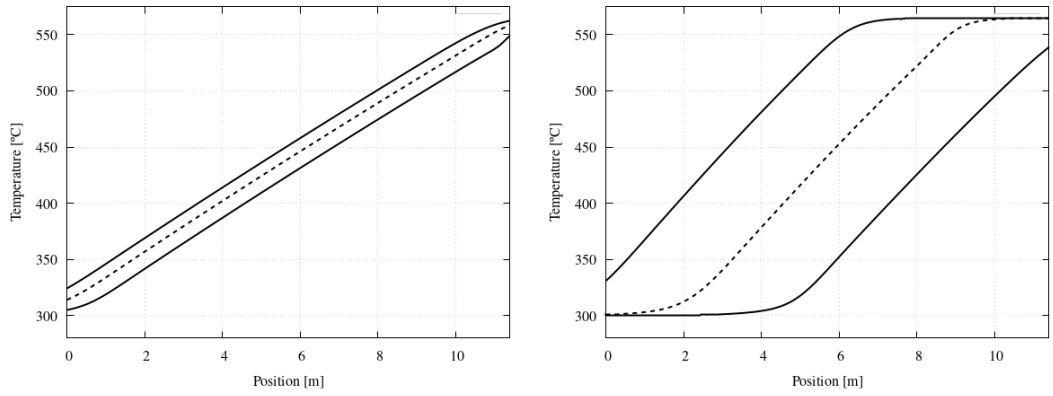

Fig. 10: Comparison of a case with low heat transfer to the solid (left) to one with high heat transfer (right).

5. Parametric results

The results of the parametric cases are shown in Table 2. The shown data correspond to a steady cycling condition, t_c and t_d are the duration of the charge and discharge cycle respectively, E_{acc} is the accumulated (or discharged) energy over a charge (or discharge) cycle, and P_c and P_d are the charge and discharge power.

Tab. 2: Results for the parametric study

#	Case	$t_c\ [h]$	$t_d\ [h]$	$E_{acc}\ [MWh]$	$P_c\ [MW]$	$P_d\ [MW]$
1	Reference case	2.1	5.1	1311	621	257
2	D=53.95m | h_{bed}=8m (const. h_{top} and h_{bot})	2.3	5.5	1411	619	256
3	D=48.25m | h_{bed}=10m (const. h_{top} and h_{bot})	2.2	5.3	1349	619	256
4	D=39.40m | h_{bed}=15m (const. h_{top} and h_{bot})	2.0	4.9	1248	621	257
2b	D=53.95m | h_{bed}=8m (const. V_{top} and V_{bot})	2.0	4.8	1222	618	256
3b	D=48.25m | h_{bed}=10m (const. V_{top} and V_{bot})	2.1	5.0	1279	619	256
4b	D=39.40 m | h_{bed}=15m (const. V_{top} and V_{bot})	2.2	5.3	1362	620	256
5	Tube diameter $d = 5mm$	1.3	3.1	786	614	254
6	Tube diameter $d = 15mm$	3.2	7.6	1960	622	258
7	Distance between tubes $L_{tp} = 15mm$	3.2	7.8	2005	623	258
8	Distance between tubes $L_{tp} = 25mm$	1.3	3.2	804	614	255
9	Square hole arrangement 90º	2.0	4.9	1264	620	256
10	Cutoff temperature $\Delta T_{co} = 30\ ºC$	4.0	9.7	2479	619	256
11	Cutoff temperature $\Delta T_{co} = 45\ ºC$	5.2	12.5	3187	616	255
12	Charge | discharge mass flow $\dot{m}_c = 744\ kg/s \mid \dot{m}_d = 307\ kg/s$	6.1	14.8	1903	312	128
13	Charge | discharge mass flow $\dot{m}_c = 2976\ kg/s \mid \dot{m}_d = 1230\ kg/s$	0.7	1.6	830	1230	509

For cases with the same mass flow rate, the charging/discharging power does not variate significantly. The accumulation of energy is defined by the duration of the cycle, which is determined by the temperature of the HTF at the outlet of the tube and the prescribed cut-off temperature.

It can also be observed that the influence of the geometrical parameters on the results is mainly due to the change in velocity. When the tube diameter increases and the mass flow is kept constant, the velocity of the fluid decreases. This means that the fluid takes longer to transport the temperature profile (while also it has more time to exchange energy with the solid), then, the cutoff temperature takes a longer time to be reached, increasing the duration of the cycle. The same effect is observed when the distance between tubes is reduced, meaning that the number of channels in the tank is greater, so the velocity decreases.

In the case of the tank diameter, if both buffer zones' heights are maintained constant, and the tank diameter increases, then the velocity will decrease and the duration of the cycle will be longer. However, if the volume of the buffer zones is kept constant, the height of these zones will change. For larger diameters, they will have less thermal inertia (than their constant height counterpart) decreasing the duration of the cycle, while for smaller diameters they will have more inertia, hence increasing the duration of the cycle.

The dependency of the accumulated energy on the velocity through a channel for the studied cases is shown in

Figure 11. In this plot, the cases for the different cutoff temperatures were neglected.

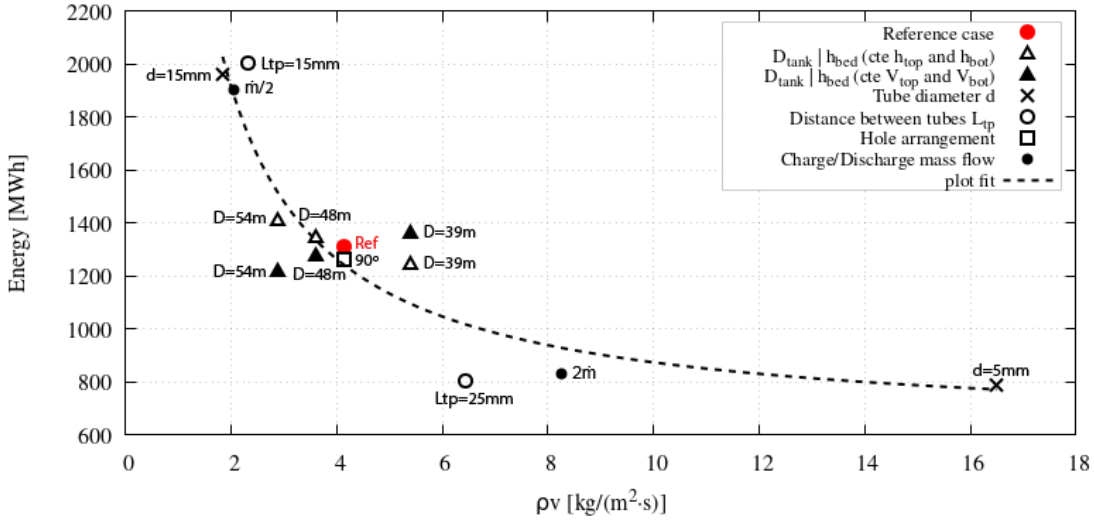

Fig. 11: Plot of the influence of velocity for the studied parametric cases (cases with different cutoff temperatures not included).

The accumulated energy trend can be modeled with an offset of some function of type $E \propto (\rho v)^{-1}$ (dashed line), although the fit is not entirely accurate for some cases, for example $L_{tp} = 25\ mm$.

6. Conclusions

A model was used to evaluate the performance of a structured type of thermocline storage tank for the accumulation of thermal energy in CSP plants. The model considers a coupled region of the fluid molten salt (1D discretization) and solid bed material (3D discretization). First, a case for a reference tank geometry was evaluated. It is observed that the capacity of thermal storage at the first cycles was greater and that is progressively reduced until it reaches the cycling periodic conditions of 1311 MWh with a charge cycle duration of 2,1h and a discharge cycle of 5,1h. Most of the energy (77%) is stored in the solid material. After that, the influence of several geometrical and operational parameters was studied. It is observed that the main difference between case results was due to the difference in fluid velocity, where this velocity is conditioned by the mass flow rate and the geometry of the tank or channels. For small velocities, the cycle is longer and the energy accumulated is greater, while for large velocities, the opposite is obtained.

Changing the diameter and height of the tank had some influence on the overall accumulation of energy, however, this influence was weak when compared to other parameters. The change in diameter and distance between tubes had a strong influence on the accumulated energy and cycle duration. If the void fraction (relation between the local volume occupied by the fluid and the total volume) increases, the energy accumulated is higher. However, more HTF is needed. In the case of the comparison of the arrangement of channels, the staggered (triangular) arrangement performed a bit better than the inline (square) arrangement, but with small differences. The increase of the buffer zone volume increases the duration of the cycles, as the HTF takes longer to reach the cutoff temperature. Also, if the cutoff temperature is increased, the system can accumulate more heat and the cycles are longer. Finally, charging and discharging power showed to be almost proportional to the mass flow rate. However, the duration of the cycles was also dependent on this mass flow rate. Even if the case of double mass flow rate had more charge/discharge power, the cycle was shorter and ended with less overall accumulated energy.

7. Acknowledgments

Newcline project is supported under the umbrella of CSP-ERA.NET 1st Cofund Joint Call and by the following National Agencies: AEI (Spain), CDTI (Spain), Jülich (Germany), SFOE (Switzerland). CSP-ERA.NET is supported by the European Commission within the EU Framework Programme for Research and Innovation HORIZON 2020 (Cofund ERA-NET Action, N° 838311).

8. References

Bonk, A., Sau, S., Uranga, N., Hernaiz, M., & Bauer, T., 2018. Advanced heat transfer fluids for direct molten salt line-focusing CSP plants. Progress in Energy and Combustion Science, 67, 69-87.

Galione, P. A., Pérez-Segarra, C. D., Rodríguez, I., Oliva, A., & Rigola, J., 2015. Multi-layered solid-PCM thermocline thermal storage concept for CSP plants. Numerical analysis and perspectives. Applied energy, 142, 337-351.

González, I., Pérez-Segarra, C. D., Lehmkuhl, O., Torras, S., & Oliva, A., 2016. Thermo-mechanical parametric analysis of packed-bed thermocline energy storage tanks. Applied energy, 179, 1106-1122.

Pelay, U., Luo, L., Fan, Y., Stitou, D., & Rood, M., 2017. Thermal energy storage systems for concentrated solar power plants. Renewable and Sustainable Energy Reviews, 79, 82-100.

J. Vera, G. Colomer, O. Sanmartí and C. D. Perez-Segarra, 2022. Modelization of a molten salt thermal energy storage for concentrated solar power. In 8th European Congress on Computational Methods in Applied Sciences and Engineering ECCOMAS 2022